

Experimental assessment of an asymmetric steel–concrete frame under a column loss scenario

G. Rovero¹, N. Baldassino^{2,*}, R. Zandonini², F. Freddi³

¹ *Caldaro s.s.d.v., Bolzano, Italy*

² *Dept of Civil, Environmental and Mechanical Engineering, University of Trento, Trento, Italy*

³ *Dept of Civil, Environmental and Geomatic Engineering, University College of London, London, UK*

* *Corresponding author. E-mail address: nadia.baldassino@unitn.it (N. Baldassino).*

Abstract

Several noteworthy accidents clearly pointed out the risk of disproportioned collapse of framed structures. Design codes recently recognized it by adding a new requirement: the structural robustness. Among the different approaches to check robustness, the most popular is associated with the column loss scenario: the analysis should verify that, in case of a column loss, an alternative load path does exist, limiting the portion of structure affected by collapse. Consequently, numerous experimental and numerical studies of 2D and 3D structures were carried out in recent years to identify the mechanism of load transfer from the damaged to the undamaged part of the structure. This knowledge becomes an essential and fundamental key for assuring adequate resistance against progressive collapse by the development of catenary action in the beams and membrane action in the floor slab. Studies of reinforced concrete systems and of bare steel sub-assemblies are numerous. More recent is the focus on the response of steel–concrete composite structures subjected to accidental events. Furthermore, most of these studies focused on the characterization of 2D sub-assemblies or 3D in-scale framed structures. This paper presents an experimental assessment of the structural response of a 3D full-scale steel and concrete composite frame under the column loss scenario. The results are finally compared with the response of a frame with the same overall geometry but different columns' layout, tested by the Authors within the same research programme.

Keywords: Progressive collapse; Column loss scenario; Framed structures; Steel-concrete composite frames; 3D full-scale test; Semi-rigid joints

1. Introduction

Progressive collapse caused by accidental actions is a fairly rare event. However, the high disruptive potential of such events calls for reliable design criteria to avoid or limit the potential economic and human costs associated with accidental scenarios.

The studies of progressive collapse started just after the Ronan Point collapse, which happened in London at the end of the 60's [1]. However, the greater boost to studies and research work was triggered by the collapse of the Twin Towers in New York City in 2001 [2]. Numerous numerical and experimental analyses were carried out to achieve an adequate knowledge of the structural performance in case of accidental loads. The main goal was to identify design criteria allowing the activation of alternative load paths associated with the redistribution of forces from the damaged to the undamaged part of the structure. Early studies mainly focused on reinforced concrete structures. The performance of composite steel–concrete frames was less investigated, despite their popularity in several countries. Recently, an increasing number of studies of this type of structures were carried out [3,4]. These studies were carried out at different levels: the component level (*i.e.*, structural members and joints) and the structural system level (*i.e.*, substructures and full structures). In particular, close attention was devoted to the joints due their central role in the mechanism of force transmission [3]. Both the individual components and the full-joint were investigated, focusing on the requisites to be met for providing the structure of adequate resources in terms of large displacements under the new stress state associated with a new load transfer system. At the structural level, quite limited are the experimental studies of the full structure: problems in terms of safety, and of economical and human resources, led to perform tests on substructures 'extracted' from full buildings [3]. The specimens were either 2D or 3D, in some case scaled down with respect to the actual building dimensions. Depending on the purpose of the test, they incorporated or not the floor system. In this context, the general and well-recognized column loss scenario was considered in most of the experimental and numerical analyses [5–7]. Moreover, few studies focussed on the contribution of the slab [8], even if it is well recognized that the concrete slab could significantly increase the ultimate resistance of many reinforced concrete (RC) structures and composite steel–concrete structures, limited research on this topic has been carried out [8]. As to RC buildings, Qian *et al.* [9] performed experimental tests on 3D concrete slab floor systems, and showed that the loads are initially resisted by flexural behaviour followed by compressive membrane action, compressive arching action, tensile membrane action and tensile catenary action. The authors concluded that, for beam-slab concrete structures, the tensile catenary and tensile membrane action developed in the beams and in the slab respectively,

significantly reducing the probability of structural collapse. Lim *et al.* [10] investigated the contribution of the concrete slab in RC structures subjected to corner column and external column removal. In the case of corner column loss, the tensile membrane action could not be developed as pointed out by the absence of the associated compressive ring. In the external column loss scenario, the tensile membrane action enabled to increase the load-carrying capacity of the slab of about 2.5 times the slab flexural capacity, enhancing the maximum frame capacity by 40 %. Further experimental and numerical studies [11–15] confirmed the important contribution of the concrete slab for the robustness of structures and the role of floor systems in redistributing the loads once a column is lost. Besides, several recent studies of steel and composite steel–concrete buildings suggested that the role of the concrete slab in progressive collapse of building is fairly complex and that it is important to consider the beneficial membrane action in design [16]. Fu *et al.* [17] conducted a 1/3 scaled test on a 3D steel-frame-composite-floor system to investigate the load-resisting mechanisms under the internal column removal. The results showed that a tensile membrane action activated within the composite floor system and that an adequate deformation capacity of the beam-to-column connections allows a ductile failure mode of the 3D floor system to be achieved. Kim *et al.* [18] developed a refined numerical model able to get the main features of the composite slab performance in presence of the loss of an external column. In a different perspective, Dimopoulos *et al.* [19] numerically studied the robustness of a seismic-resistant steel–concrete composite building using self-centering moment resisting frames. The results showed that the building can withstand the code-prescribed load with a safety factor of 2 and that the structural limit state that triggers progressive collapse is the buckling of the gravity columns.

The robustness of composite steel–concrete frames affected by accidental actions was deeply studied in the European RFCS Research Project ‘ROBUSTIMPACT (Robust impact design of steel and composite building structures) [20]. This European research project aimed at developing a new robust design approach against impact loading based on the column residual strength and the alternate load path method. In this framework, the University of Trento conducted two 3D full-scale tests on composite steel–concrete subframes subjected to column removal. The tests allowed investigating the redundancy of the structures and the alternate load paths provided by the floor system. The need of the beam-to-column connections to sustain important rotations under a combined stress state and of a concrete slab to develop membrane effects was pointed out. The tests simulated the response of two full-scale sub-frames extracted from reference buildings as described in detail in [4]. The frames were characterized by the same overall dimensions, materials and structural members, but by a different column layout. In particular, in the first tested frame, the columns were positioned symmetrically with respect to both the directions, while in the second the symmetry was in the longitudinal direction only. This difference enabled to assess the influence of the uneven stiffness of beams and slabs in contiguous spans. The two frames were named as ‘symmetric’ and ‘asymmetric’ frame, respectively.

The outcomes of the test on the ‘symmetric’ frame were presented and discussed in [4] together with the main features of the experimental study. The test on the ‘asymmetric’ frame is here described, its results reported and then compared with the previous test in order to single out differences and similarities.

2. The tests in Trento

2.1. The case study frames

The one floor sub-frames tested in the laboratory were extracted from the first floor of a reference five-storey building as described in detail in [4]. The case study is a five storeys composite steel and concrete framed structure designed according to Eurocodes [21–25]. No consideration was made for the accidental loads (*i.e.*, seismic and associated to robustness). The structural design led to select HEB220 for the columns, IPE240 for the beams and a thickness of 150 mm for the concrete slab. The connection between steel beams and concrete slab was designed as full shear connection. A welded wire mesh of $\phi 10/150 \times 150$ mm was located at the bottom and top side of the slab, while additional reinforcing bars were required in several zones [26]. Beam-to-column joints had bolted flush-endplate connections designed according to the component method [25]. Concrete C30/37, rebars grade B450C, structural steel grade S355 and bolt class 10.9 were selected for the materials of the structural elements. While these features were the same for the two buildings object of the study [26], the columns’ layout was different, leading to a ‘symmetric’ and a ‘asymmetric’ case. Fig. 1 shows the plan view of the reference frame for the asymmetric case: the hatched shaded area identifies the substructure for the current study.

The main focus of the second test was the investigation of the asymmetry’s effects in a frame subjected to an internal column loss. In other terms, the two tests were designed to allow investigating the influence of the ‘slab parameter’. Referring to the ‘symmetric’ test [4], at the end of the central column removal the load redistribution from the damaged to the undamaged part of the structure occurred almost symmetrically, as it was pointed out

also by the torsional rotation of the lateral beams. A cracking pattern typical of slabs where membrane forces were activated was observed.

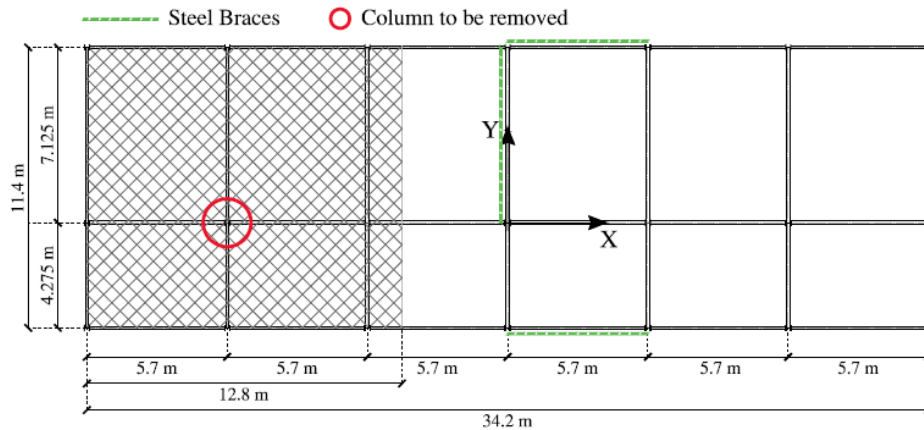


Figure 1. Plan view of the reference structures: the asymmetric case.

2.2. The 'asymmetric' sub-frame

Fig. 2 illustrates the plan and sectional views of the sub-frame specimen. The design of the set-up required an accurate selection of the restraining system details reproducing the interaction with the remaining part of the reference structure [26]. To this aim a number of numerical simulations were carried out of the overall reference frames and of the full-scale specimens. The outcomes allowed for sizing the sub-frames restraining system and pointed out the need for extending the subframes columns above the floor and for connecting them at the top with truss sections (see also Fig. 3).

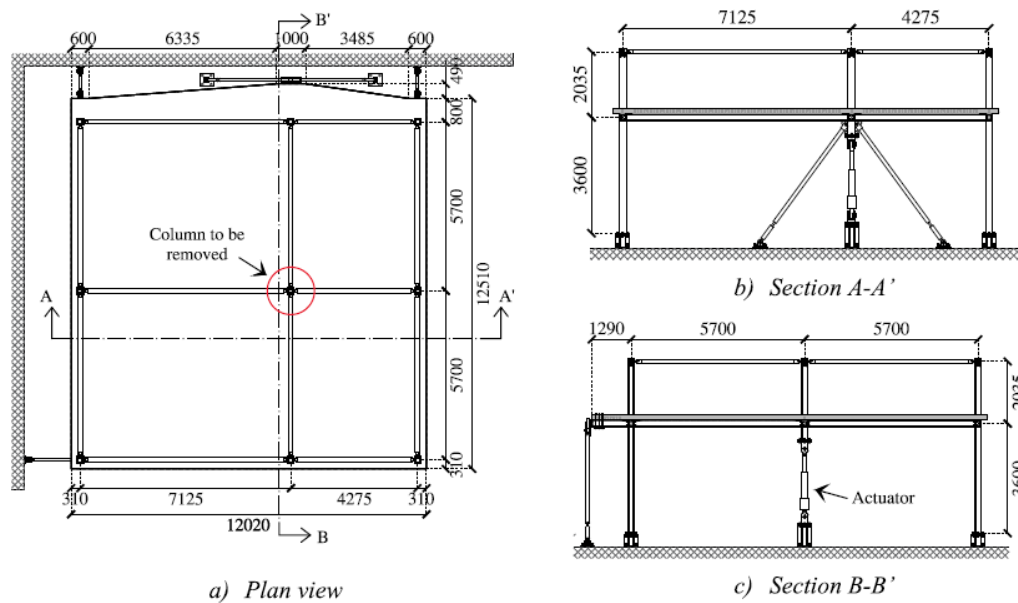


Figure 2. Plan view and cross sections of the asymmetric sub-frame (measures in mm).

As to the restraining system, suitable connections to the counter walls and to the strong floor of the laboratory were designed [26]: the sub-frame was connected to the counter-wall by horizontal trusses (br. A2, br.G2 and br.I2) in order to prevent horizontal displacement, and to the strong floor by a truss system (br.H2) in order to prevent vertical displacement (Fig. 3). During the test, the collapse of the central column, 'replaced' by a hydraulic actuator (Fig. 3), was simulated. Before the beginning of the test, the load acting on the 'actuator' was carried by a provisional propping system that was removed once the jack was activated.

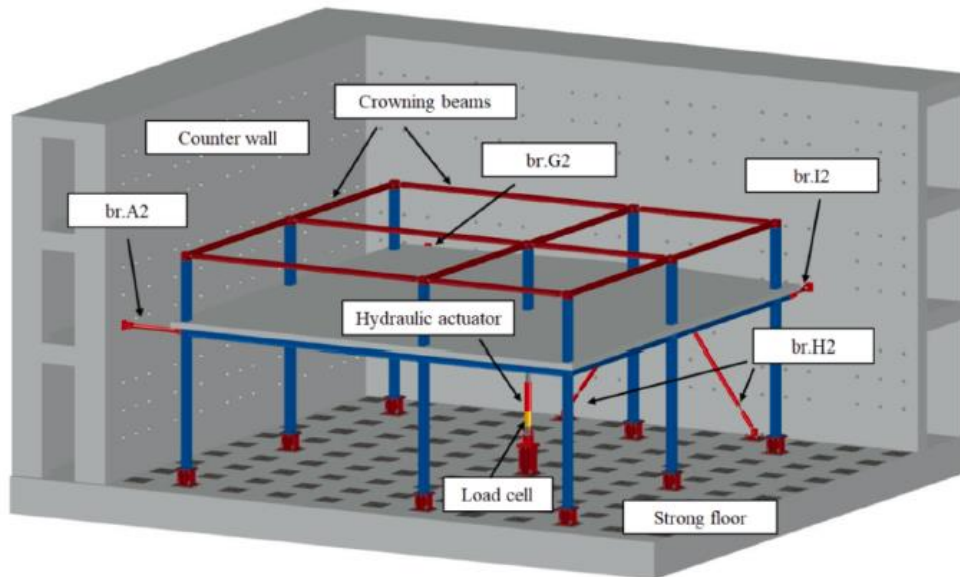


Figure 3. The specimen and the test set-up.

2.3. Building the specimen

The specimen was built inside the Laboratory of Materials and Structures Testing of the University of Trento. At first, the steel skeleton was erected connecting the columns with the strong floor of the laboratory and the lateral bracing system with the counter-wall (Fig. 4a). After the installation of the formwork (Fig. 4b), the reinforcement was positioned and the slab casted in three phases (Fig. 4c).



a) Steel skeleton erection

b) Formwork installation

c) Concrete casting

Figure 4. The constructional phases.

2.4. Materials

Samples were prepared for the mechanical characterization of the materials in accordance with the relevant standards.

2.4.1. Concrete

During the pouring, 13 concrete cubes and 5 cylinders were taken from each the three concreting casts, with a total of 39 cubes and 15 cylinders. In order to get an appraisal of the influence of the curing conditions, 18 cubes were cured following the prescription of the EN 12390-2 [27], and 21 cubes were cured in air. All the cylinders were cured following the prescription of the EN 12390-2 [27]. Compression tests on cubes and splitting tests on cylinders were performed as prescribed by the EN 12390-3 [28] and by the EN 12390-6 [29], respectively. In order to appraise the increase in time of the concrete compression strength, tests on cubes were performed at the age of 8 days, 33 days and 111 days (*e.g.*, the time of the full-scale test) from casting. Splitting tests on the cylinders were conducted at the age of 33 days and 111 days. The cylinders tested at the time of the test (*i.e.*, 111 days), preliminary to the splitting tests, were used for the evaluation of the modulus of elasticity of the concrete in accordance with [30]. The average value of the modulus of elasticity was of 21070 MPa. The results of the tests, reported in Table 1, indicate that the curing conditions did not affect the concrete resistance in compression. The average cube compressive strength of the concrete at the time of the test exceeds the average nominal value of about 51 %. A similar increase was found in the ‘symmetric’ frame [4].

Table 1. Concrete properties.

Type of test	Concrete age (days)	Curing conditions	n. of tests	Average cube compressive strength (MPa)	Average tensile splitting strength (MPa)
Compression test	8	EN 12390-2	3	45.91	–
		Air	3	42.47	–
	33	EN 12390-2	9	54.48	–
		Air	9	53.69	–
	111	EN 12390-2	6	57.59	–
		Air	9	57.34	–
Splitting test	33	EN 12390-2	6	–	3.69
	111	EN 12390-2	9	–	4.16

2.4.2. The Steel

Mechanical properties of the steel, obtained from tensile tests, are summarized in Table 2 and Table 3 for the reinforcement bars and for the structural steel, respectively. The mechanical properties of the steel are in accordance with the design values described in Section 2.1, except for the steel of column HEB220 whose average yield stress is lower of about 15 %.

Table 2. Mechanical properties of the reinforcement bars.

Rebars diameter (mm)	Yield stress R_e (MPa)	Tensile strength R_m (MPa)	Ratio R_m/R_e	Ratio $R_e/R_{e,Nom}$	Agt %
10	496	586	1.18	1.10	10.5
16	523	631	1.21	1.16	9.4

Table 3. Mechanical properties of the structural steel.

Component	Yield stress (MPa)	Average yield stress (MPa)	Ultimate tensile strength (MPa)	Average ultimate tensile strength (MPa)	Fracture strain A (%)
Column HEB 220	300	303.3	441	440.3	34.9
	306		442		34.5
	304		439		36.1
Beam IPE 240	383	409.3	537	540.7	28.2
	391		541		27.0
	454		544		33.3
Endplate 10 mm	373	371.7	562	559.0	32.6
	370		560		33.1
Strong direction	372		556		35.4
Endplate 10 mm	382	381.3	558	558.0	30.9
	380		559		30.8
Weak direction	382		557		26.0

2.5. The measurement set-up

The behaviour of the frame was monitored by measuring deformations, displacements and rotations of the main structural elements. An accurate selection of the key parameters to be measured during the test was conducted. Moreover, the results of the first ‘symmetric’ test made possible to improve the instrument set-up allowing a more effective information of the response to be achieved. The instrumentation set-up was installed as illustrated in Figs. 5–7.

In particular, all the columns in the asymmetric frame were instrumented with strain gauges at the base in order to comprehensively assess the redistribution of the gravity loads, whereas in the first test the columns instrumented were five out of eight. Furthermore, more attention was paid to the joints between the removed column and the beams. Strain gauges were installed on the upper and lower beam flanges at a distance of 210 mm from the beam end. Further strain gauges were installed in the bolts of the central node.

Within the assumption of elastic material, the strain gauges readings enabled determination the axial force and/or the bending moments acting on a structural element. Fig. 5 identifies the position of the strain gauges in the frame: i) the columns (Fig. 6a and b) were instrumented at the base to measure the average axial strain and the curvature about the strong and weak axis; ii) strain gauges were installed in the internal beams (Fig. 6c) and d) in correspondence of the beams’ mid-span and near the central column E2 enabled determination of the axial strain and the curvature about the strong axis; iii) all bolts of the joints that connect the internal beams with the central column E2 were instrumented and calibrated with strain gauges to measure the axial strain state during the test; iv) strain gauges were also installed in several reinforcement bars close to the central column as illustrated in Fig. 7, in the lateral restraining members and in the crowning beams. Displacement transducers (linearity 0,1 %

F.S. – resolution $< 1 \mu\text{m}$) and inclinometers (linearity deviation $< 1 \times 10^{-3}$ F.S. – resolution $< 1 \times 10^{-3}^\circ$), installed in correspondence of the beam-to-column connections, allowed monitoring the joints rotation. Further LVDTs at the mid-span of the external beams AB2, BC2 and CF2 (Fig. 5) allow measuring the torsional rotation, and on the external columns, at the beams level, enable determination of the columns' rotation. The vertical displacement of the central points of the slab panels and of the central node were monitored by using wire transducers. Furthermore, a load cell (max capacity of 1MN – class 0.5 according to EN ISO 376 [31]) coupled with the hydraulic actuator measured the force acting on the central column E2. Table 4 summarizes the instruments, the parameters directly measured, and the ones determined indirectly.

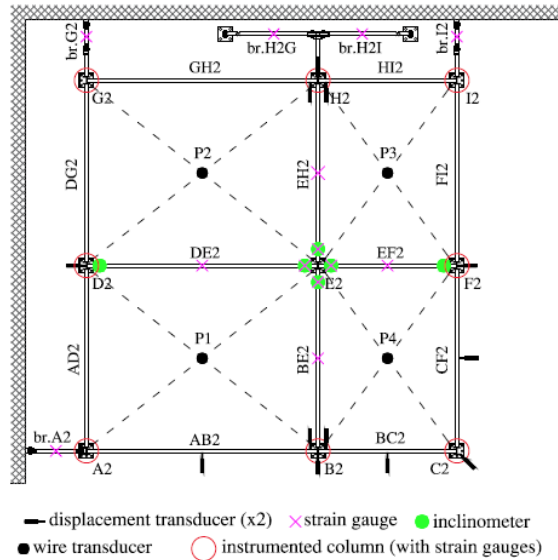


Figure 5. The instrumentation set-up.

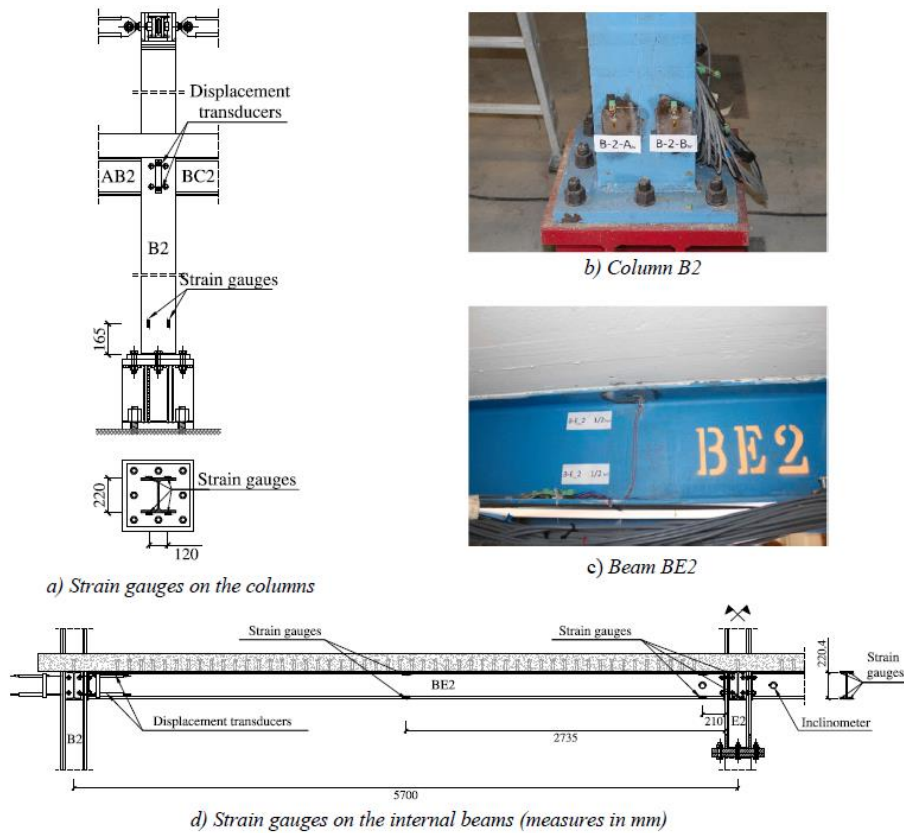


Figure 6. Strain gauges on the steel members.

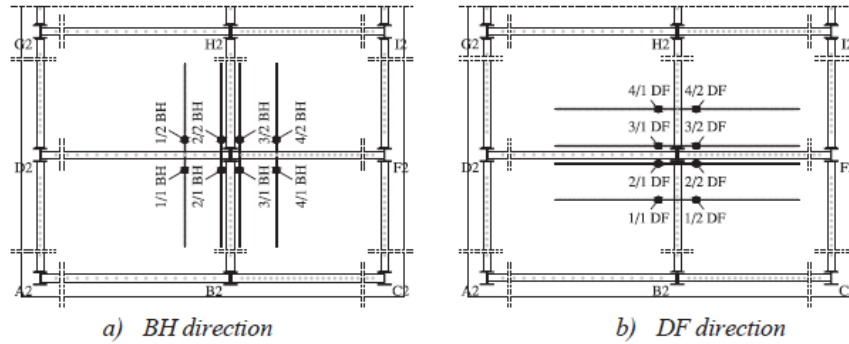


Figure 7. Strain gauges on the reinforcement bars.

Table 4. Mechanical properties of the structural steel.

Structural element	Instrument	Parameter measured	Parameter deducted
Columns	Strain gauges at the base	Average axial strain	Axial force
		Curvature (strong and weak axis)	Bending moment
		Displacement transducers at the beam level	Rotation
Central beams	Strain gauges at mid-span and near the central column	Average axial strain	Axial force
		Curvature (strong axis)	–
Lateral beams	Displacement transducers at mid-span	Torsional rotation	–
Crowning beams	Strain gauges at mid-span	Axial strain	Axial force
Lateral restraints	Strain gauges at mid-span	Axial strain	Axial force
Reinforcement bars	Strain gauges near the central column	Axial strain	Axial force
Bolts of the central joints	Strain gauges	Axial strain	Axial force
Joints	Displacement transducers	Rotation	–
	Inclinometers	Rotation	–
Slab panels	Wire transducer	Vertical displacement	–
Hydraulic jack	Load cell	Axial load	–
	Wire transducer	Vertical displacement	–

2.6. The testing phases

The following testing procedure was adopted:

- phase 0: activation of the actuator and removal of the propping system that sustained the loads during the constructional phases (Fig. 8a); reading of the axial force on ‘column E’ due to the gravity load;
- phase 1: application of the live loads onto the slab by using sand filled bags (Fig. 8b). The bags were placed on the slab in two layers: the first one was uniformly distributed on the whole surface of the slab (153.26 m² - total load of 932.14 kN), while the second one was applied on a reduced area (74.60 m² - total load of 392.22 kN) as illustrated in Fig. 9. The total live load was hence of 1324.36 kN;
- phase 2: simulation of the column removal by letting the hydraulic pressure of the actuator to freely decrease down to zero;
- phase 3: after a stabilization period, application of a tensile force at the central node by means of the hydraulic jack increased up to the ‘collapse’, in order to get an appraisal of the residual strength of the specimen.



a) The actuator and the propping system



b) The specimen under full gravity loading

Figure 8. Test phases.

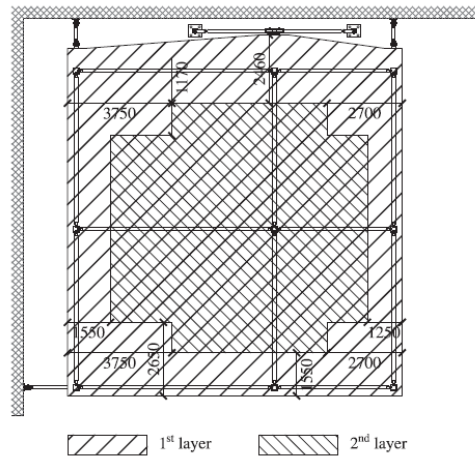


Figure 9. The loading layout.

The load applied in phase 1 reproduces the uniform factored design load at the ultimate limit state (ULS) of 9.0 kN/m^2 , so simulating the most adverse condition before the column collapse. The duration of the test, comprising all the testing phases from the removal of the propping system to the ‘collapse’, was of about 28.5 h. The instruments data were logged with a frequency of 2 Hz.

3. Experimental results

3.1. Global behaviour and failure modes

The overall response can be illustrated by means of the relationship between the axial load NE2 on the ‘central column’ and the vertical displacement at this column, as in Figure 10. In the graph, compression is positive, while tension is negative. As a first general remark, the continuity of the curve suggests that the flexural behaviour contributes the most to the response even in the last phase.

The analysis of the response highlights the testing phases and the corresponding values of the load and deflection at the end of each phase, as reported in Table 5.

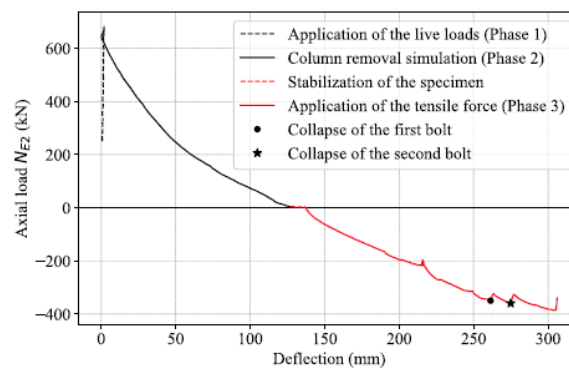


Figure 10. Load-deflection response.

Table 5. Load-deflection values.

Testing phase	Load [kN]	Deflection [mm]
End of propping system removal	250.39	0.00
End of loading phase	681.23	1.15
End of column removal	4.44	126.70
End of stabilization phase	2.90	136.80
Collapse of the 1 st bolt	-349.62	261.38
Collapse of the 2 nd bolt	-359.45	274.89
End of the test	-386.30	303.64

At the end of the propping system removal (phase 0), the vertical reaction force on the ‘central column’, associated with the self-weight of the structure, was equal to 250.39 kN. The application of the live load onto the slab (phase 1) increased the reaction force to 681.23 kN, with a vertical displacement of 1.15 mm.

The column removal (phase 2) was simulated leaving the hydraulic pressure of the actuator freely decreasing up to the condition of no axial load, which was associated with a vertical displacement of 126.70 mm. After a stabilization phase, during which the deflection increased up to 136.80 mm, a tensile force was applied to the central node by the actuator (phase 3). When the deflection of the central node reached 261.38 mm with a corresponding value of the reaction force of -349.62 kN, the rupture of a bolt in the bottom row of the steel joint between the central column E2 and the beam EH2 occurred. The reaction force was further increased up to -359.15 kN when the adjacent bolt in the same joint collapsed. The associated vertical displacement was of 274.89 mm. The test then continued up to a load of -386.30 kN and a deflection of 303.64 mm. The significant plastic deformation of the connections between the central column and the internal beams (Fig. 11a) and the local state of ‘distress’ of the concrete slab (Fig. 11b–d) and of the steel beams at the central node and at the mid-external columns (Fig. 11e) suggested to consider the collapse achieved, and to stop the test.

As a further behavioural index, the load–deflection curves at the middle of the four slab panels are plotted (Fig. 5, Fig. 12), which point clearly out the structural asymmetry.

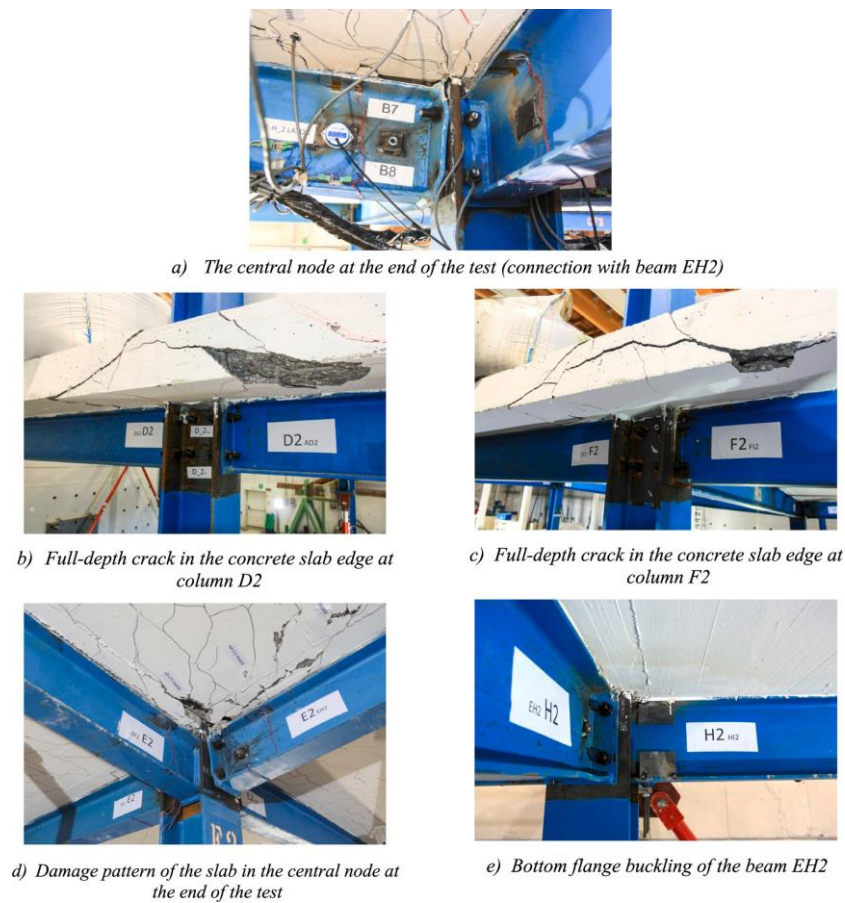


Figure 11. Critical components.

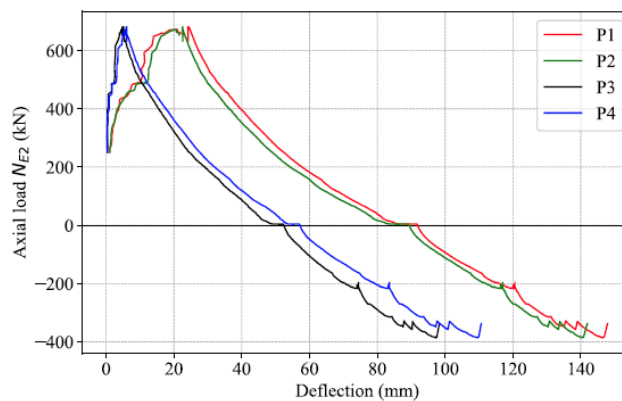


Figure 12. Vertical displacement of the slab panels.

3.2. Local behaviour: the frame components

The instruments installed in the structural members, as well as the visual observation, allow determining the behaviour of the frame components, and taking considerations about the effect of the structural asymmetry. In particular, the results reported in this section focus on the response of the columns, of the beam-to-column joints and of the slab.

Further results related to the lateral beams, to the lateral frame restraints and to the rebars are illustrated and commented in the following section. The results on other frame components, such as the central steel beams, do not show important differences with respect to the results reported in [4, 32] for the symmetric frame specimen.

3.2.1. The columns

As a first assessment of the local structural behaviour, Fig. 13a shows the evolution of the curvature at the column base of the mid-external columns B2, D2, F2 and H2, normalised on the yield curvature χ_y depending on the bending associated with the continuity with the internal beams, *i.e.*, about the strong axis for columns B2 and H2 and about the weak axis for columns D2 and F2. In the transverse direction, at the end of the loading phase 1 (*i.e.*, application of the live load onto the slab) the column D2 curvature is far greater than that of column F2, due to the different span length of the adjacent beams. Vice versa, at the end of the test, column F2 exhibits a curvature more than twice that of the opposite column D2, as a result of the central joints inelastic deformation.

In the longitudinal direction, the restraining system adjacent to column H2 (br.H2) causes the substantial difference between the curvatures of the columns B2 and H2. If the rotation of the columns at the beam level (Fig. 14a) is considered, similar conclusions can be drawn as for the base curvatures. Interesting to note that the rotation of the corner column C2 is almost negligible throughout all the test.

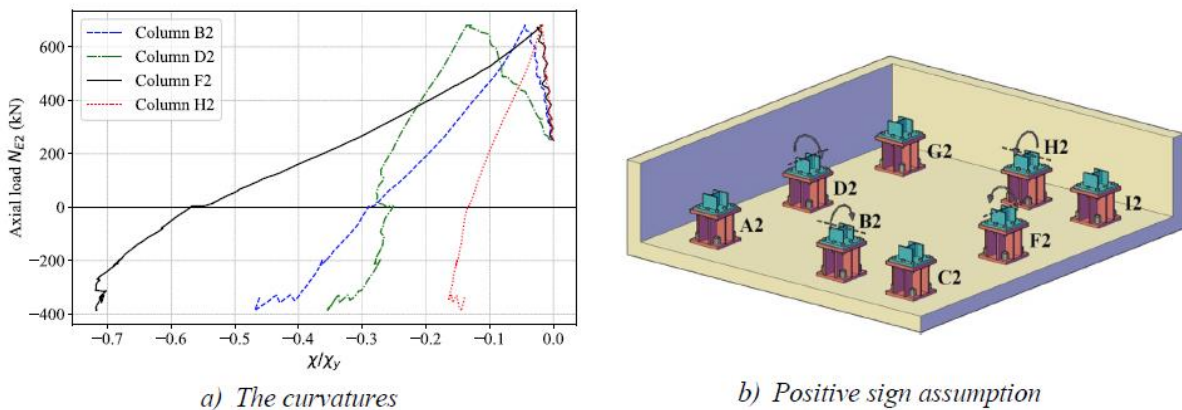


Figure 13. Curvature of the perimeter columns at the base.

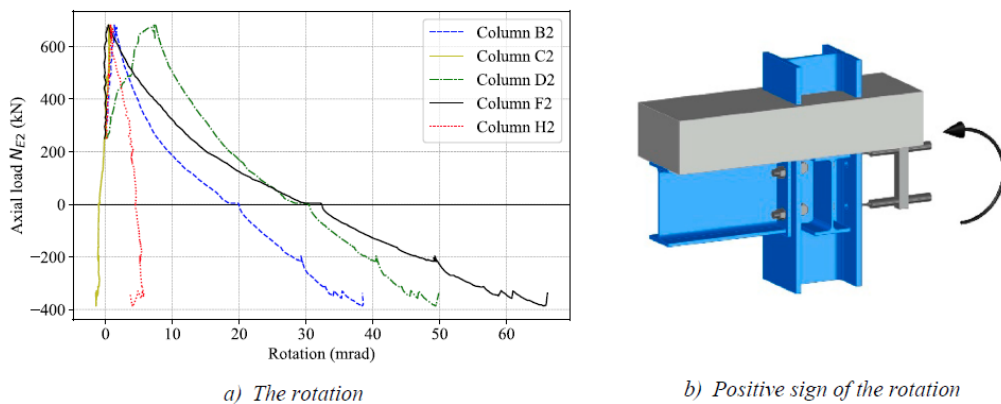


Figure 14. External columns rotation at the beam level.

The column loss triggers a redistribution of the axial load in the surrounding columns. An appraisal of the vertical loads' redistribution is provided by Table 6, where the axial forces at the columns base (computed on the basis of the strain gauges' readings and the nominal value of the area of the column cross-section) are reported.

At a first analysis of the table, corner columns A2, C2, G2 and I2 are the least stressed and no important variation in terms of their axial force during the column removal occurred. To be noted that the corner columns unloaded due to the effect of the concrete slab action: column C2, in compression at the end of phase 1, was in tension at the end of the column removal, and no further change occurred up to the end of the test. As to the mid-external columns: i) due to the nearby restraining system (br.H2), the axial force in column H2 was the highest in all phases, ii) column B2 at the end of phase 2 carried about twice the force acting before the column removal, and further increased up to 411.70 kN at the end of the test, iii) due to the frame transverse asymmetry columns D2 and F2 behave fairly differently: at the end of the test, column F2 carried more than four times the force acting at the end of the phase 1, while column D2 did not even double the force acting before the column removal. The transfer mechanism mainly happens in the longitudinal and transverse directions, while the corner columns, located along the floor diagonals are slightly affected.

Table 6. Axial forces in the columns (kN): asymmetric test.

Column	End of the loading phase (phase 1)	End of the column removal (phase 2)	End of the test (phase 3)
A2	61.62	42.94	50.78
B2	168.92	345.74	411.70
C2	32.79	-4.75	-4.65
D2	170.88	287.58	324.66
E2	681.23	4.44	-386.30
F2	98.02	314.27	423.27
G2	40.19	27.60	42.38
H2	212.31	542.48	643.19
I2	46.11	21.85	30.31

3.2.2. The beam-to-column joints

A further index of the influence of the structural asymmetry comes from the analysis of the beam-to-column joints rotation. For clarity, Fig. 15 provides the joints nomenclature and the positive sign of rotation. The responses of the four central joints are gathered in Fig. 16. The sign reversal of the rotations associated with the column removal is apparent, leading to the change from hogging to sagging bending moment in the connections. The rotations of the joints j.ED2 and j.EF2 (Fig. 16a) are quite different due to the transverse asymmetry of the frame. In particular, joint j.EF2 kept unchanged the sign of the rotation (hogging bending moment throughout the test), while the change from hogging to sagging bending moment is well experienced by joint j.ED2. On the contrary, the rotations of the joints j.EB2 and j.EH2 (Fig. 16a) are close to each other during all the test. The plastic deformation of the endplates was the main source of rotation of these joints (Fig. 11a). As to the external joints (Fig. 16b), consistent responses to the ones of internal joints can be observed. In particular, the joints in the transverse direction (with columns D and F) experience the highest rotations. As expected, the lateral joints showed a continuous increase of the rotation, leading to hogging bending moments in the connections during all the test. The curve related to joint j.HE2 is interrupted before the end of the test due to the buckling of the bottom flange of the beam (Fig. 11e) that compromised the proper operation of the instruments. It should be noted that the flange buckling lead to an ‘unloading’ of the joint.

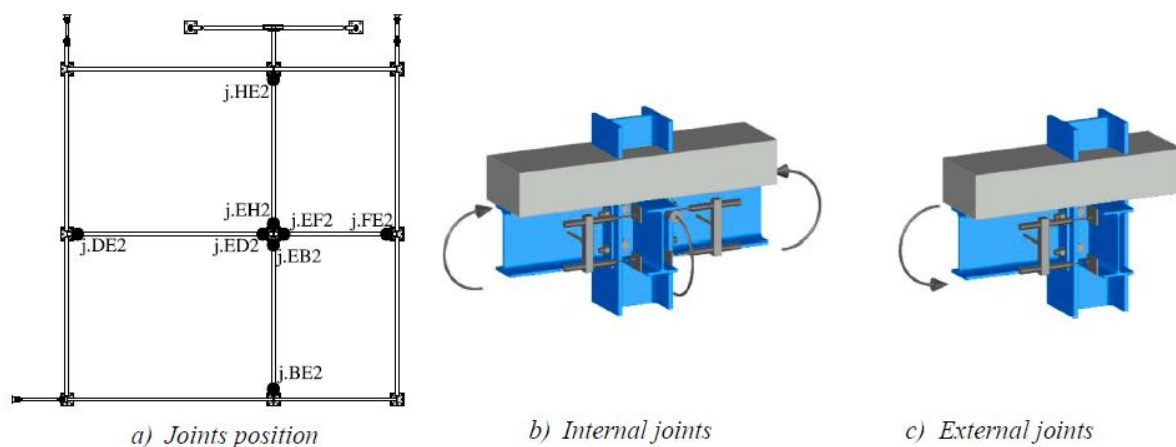


Figure 15. Joints and positive sign of the rotation.

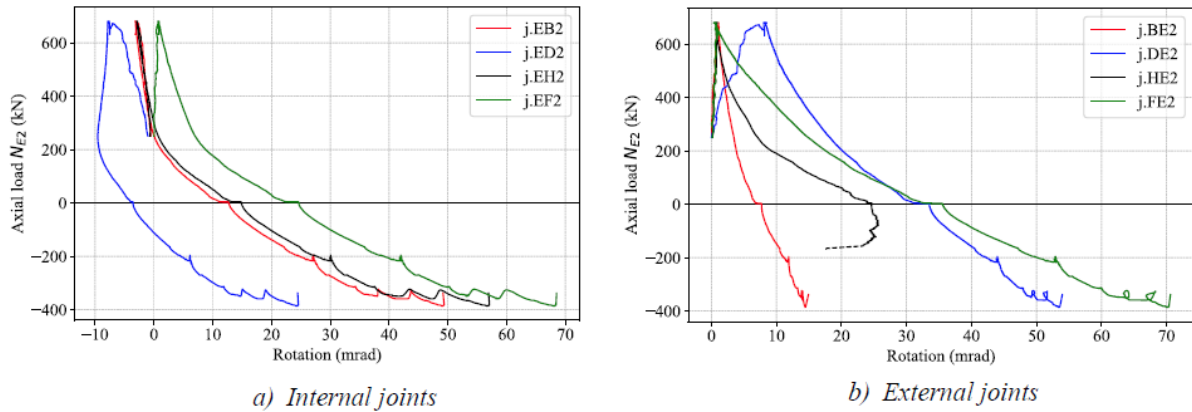


Figure 16. Joints rotation.

In the central node, eight bolts were instrumented in the longitudinal direction where the beams were connected to the column flange (bolts B1–B8) and four bolts in the transverse direction (A1–A4) connecting both beams to the column web. Fig. 17 illustrates the central joint, identifying the instrumented bolts position (Fig. 17a) and the strains in the bolts (Fig. 17b and d) normalised with respect the nominal yield deformation ($\epsilon_y = 4500 \mu\epsilon$). The bolts were tightened according to the Eurocode 3-1-8 [25]. In all bolts negligible axial deformations were measured in the loading phase (Phase 1): they were in the compression zone below the neutral axis. The unloading associated with the column removal led to the reversal of the flexural moment, and the bolts entered in the tension range. Consistently, the bottom bolts were significantly more strained. At the end of the test, the yield axial deformation of the bolts was widely exceeded by all the bolts of the bottom rows. These strains combined with the bending due to the endplate deformation caused the fracture of bolts B7 and B8 (note that the strain gauge in bolt B7 stopped working at the end of Phase 2 (Fig. 17c).

3.2.3. The slab

The evolution of the cracking pattern during the test revealed the slab role in the various loading phases: i) after the column loss, cracks on the bottom side were positioned along the diagonals of the four slab panels; ii) at the end of the test, concentric compressive rings on the top side of the slab, typical of slabs where membrane forces start to be activated, were observed.

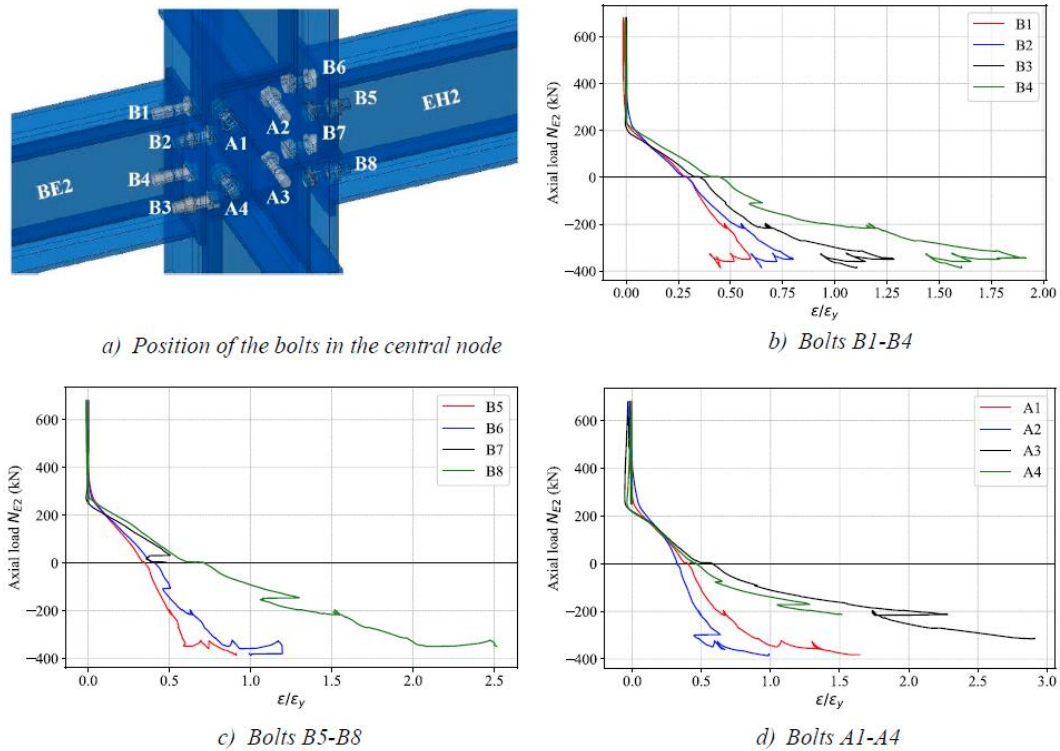


Figure 17. Axial strain of the bolt in the central node.

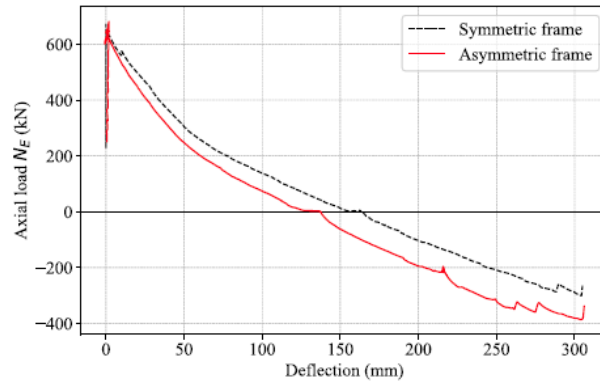


Figure 18. Comparison of the load–deflection response.

4. Asymmetric vs symmetric frame

The comparison of the quantitative results and the visual inspection during the tests of the asymmetric and symmetric [4] frames allow an insight into differences and similarities in the response mechanisms. The overall structural behaviour of the two tested frames was fairly similar as apparent from the load–deflection relationships of the central node (Fig. 18). In particular, the deflection at the end of the test is very close (303.64 mm and 304.30 mm in the asymmetric and symmetric sub- frame, respectively). However, some dissimilarities can be pointed out as the stiffer response of the asymmetric frame throughout all the loading history. This also implies a higher residual strength: the tensile force applied by the actuator to the central node at the same deflection of about 300 mm was of 386.30 kN in the asymmetric case and of 300.85 kN in the symmetric one.

As to the components' behaviour, the critical role of joints' ductility is confirmed: both tests achieved the collapse due to the fracture of two bolts in the bottom row of joint j.EH, connecting the internal beam EH to the central column E. Furthermore, plastic deformations and local phenomena, such as the local buckling of the bottom beam flange and the web shear deformation of the column web panel, were observed in the external joints in both tests.

The axial forces at the base of the columns B, C, D, E, F and H instrumented in both tests, are reported in Table 7 and Fig. 19 for the three testing phases. In the figure, the position of 'column E' is also reported for reading clarity.

Differences in the load redistribution among the columns during the test are apparent. In phase 1, the behaviour of columns B and H was fairly similar, while columns D and F exhibited a fairly different response. At the end of the loading, the load on the actuator was almost 'equal' in the two tests. However, the transverse asymmetry in test 2 led to an axial force, in column D (Fig. 19a) about 70 % greater than the force in the column F. On the contrary, forces in these columns in the first symmetric test are almost equal. These differences between the two frames tends to disappear during the second phase (Fig. 19b), and similar thrusts were observed at the end of the column removal. At the end of the test (Fig. 19c), column F in the asymmetric frame carries more load than the same column in the symmetric one. Inelastic phenomena, such as slab cracking and steel yielding partly counteract the effect of the asymmetry. On the other hand, the corner column C exhibited a quite different behaviour between the two tested frames, confirming the role of the concrete slab for the load redistribution. In the symmetric specimen, the column C unloaded and reloaded during the phases 2 and 3 respectively, while in the asymmetric one the axial force passed from compressive to tensile during the column removal, and kept this value during the application of the tension force (phase 3).

Table 7. Axial forces in the columns (kN): asymmetric vs. symmetric.

Column	End of the loading phase (phase 1)		End of the column removal (phase 2)		End of the test (phase 3)	
	Test 2	Test 1	Test 2	Test 1	Test 2	Test 1
B	168.92	143.82	345.74	319.08	411.70	373.08
C	32.79	58.01	-4.75	49.49	-4.65	63.01
D	170.88	148.99	287.58	285.07	324.66	330.83
E	681.23	669.25	4.44	2.81	-386.30	-300.85
F	98.02	151.63	314.27	308.4	423.27	365.02
H	212.31	212.07	542.48	546.84	643.19	635.54

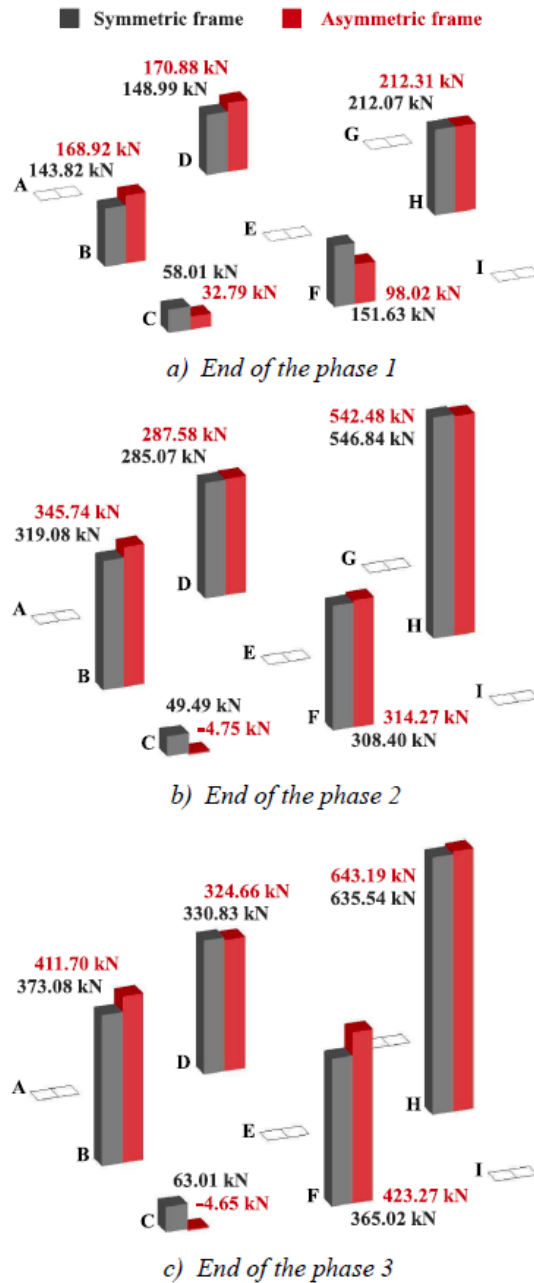


Figure 19. Comparison of the axial force at the columns base.

The influence of symmetry and asymmetry can also be highlighted by comparing the curvature at the base of the columns D and F (Fig. 20a) and of the rotation at the beam level of the same columns (Fig. 20b). As to the curvatures, there is a clear trend to build up higher deformations in column F (connected to the shorter beam) in the asymmetric test, when the central column is lost.

Joints play an important role in the load transfer when a column is lost and are the key elements to make the alternate path develop. Significant differences between the two tested frames can be observed (Fig. 21). As illustrated in Fig. 21a the internal joints j.ED and j.EF in the asymmetric specimen exhibited a fairly different response since the very beginning of the test, with joint j.EF experiencing positive rotation since the first phase. Besides, joint j.EF was demanded a fairly higher rotation, which became more than double at collapse. In the longitudinal direction (Fig. 21b), where both frames are symmetric, the internal joint responses are close to each other, with joint j.EH deforming the most.

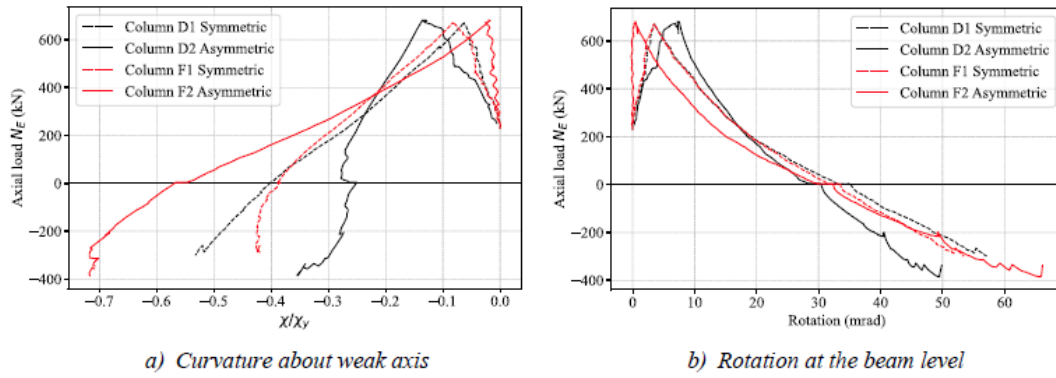


Figure 20. Measurements in the columns D and F.

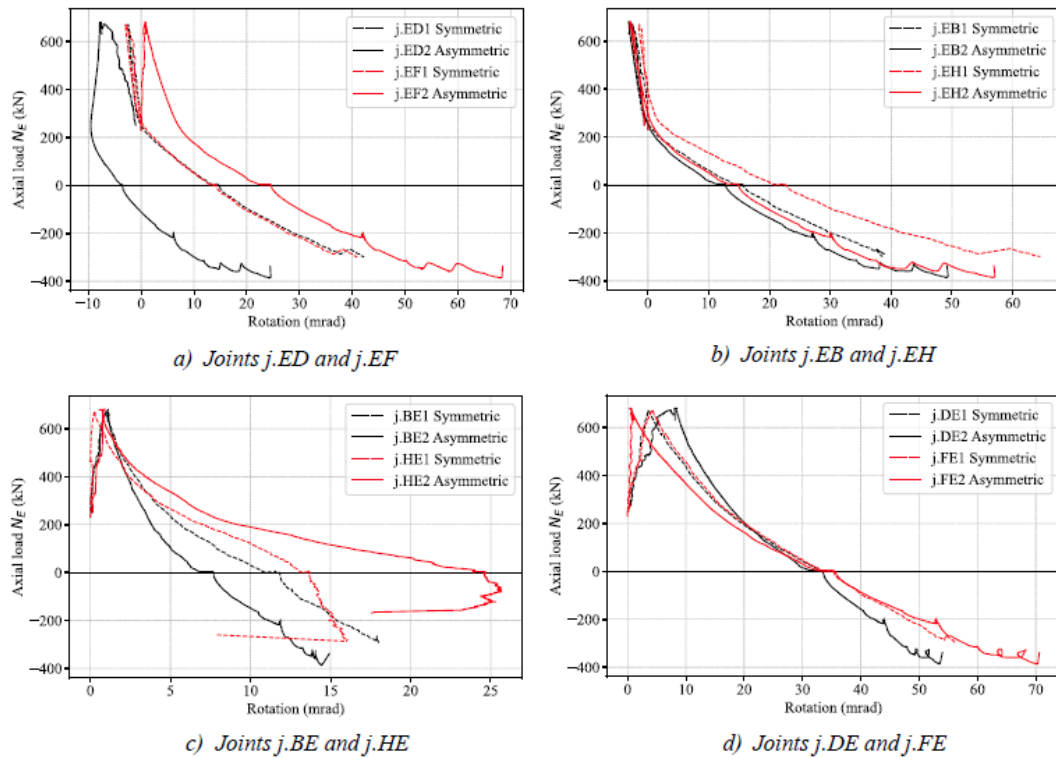


Figure 21. Comparison of the joints rotation.

The analysis of the external joints' rotations, reported in Fig. 21c and Fig. 21d, points out that in both tests the ductility demand is more significant in the transverse direction, with joint j.FE in the asymmetric frame achieving the greatest rotation at collapse. In the longitudinal direction, the buckling of the beam EH bottom flange at column H, common to both tests, is highlighted by the response of joint j.HE (Fig. 21c), which, in the second test, experiences a significant rotational reverse.

The rebars strains (Fig. 7) show the influence of the asymmetry on the concrete slab response near the central joint. The curves in Fig. 22 show that: i) all the rebars are in tension since the beginning of the test (hogging bending moment); ii) during the phases 2 and 3, the rebars in both tests showed first an unload and then a reload, with greater strains in test 2; iii) in test 2 the strains were built up dramatically and the rebars yielded in the vicinity of 'collapse'.

As to the lateral beams, the different slab's configuration resulted in a greater torsional rotation of the beams in the symmetric frame compared to the one in the asymmetric frame as illustrated in Fig. 23, for beams BC and CF. However, the general behaviour of the lateral beams was analogous between the two tested frames.

The behaviour of the lateral frame restraints showed modest axial forces, with very close values in restraints br.G and br.I in both the tests. On the other hand, the effect of the asymmetry on the torsional response of the frame is apparent from the significantly higher force in the restraint br.A. (Fig. 24).

Finally, the concrete slab: the response of both specimens showed its significant contribution to the resistance of the frames subjected to column removal. The axial strains and curvatures of the central beams, as described in [4], and the visual inspection of the cracking pattern of the concrete slab, illustrated in Fig. 25, show how 2D membrane effects started to be activated in both specimens.

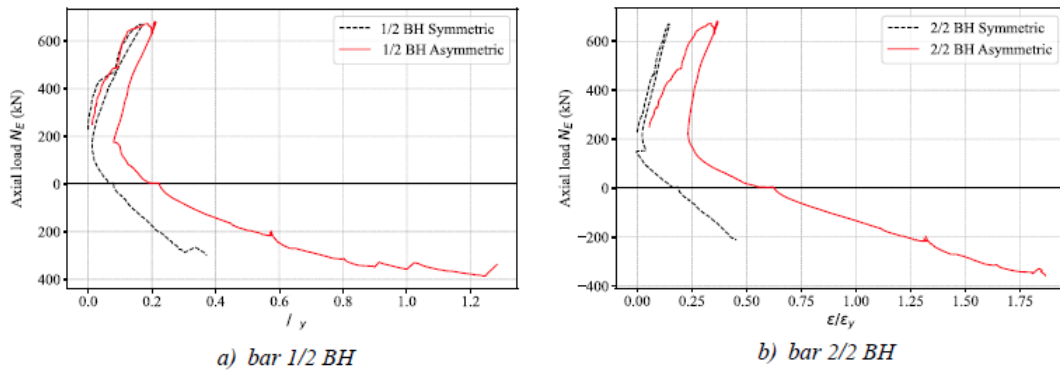


Figure 22. Comparison of the axial strain of the bars.

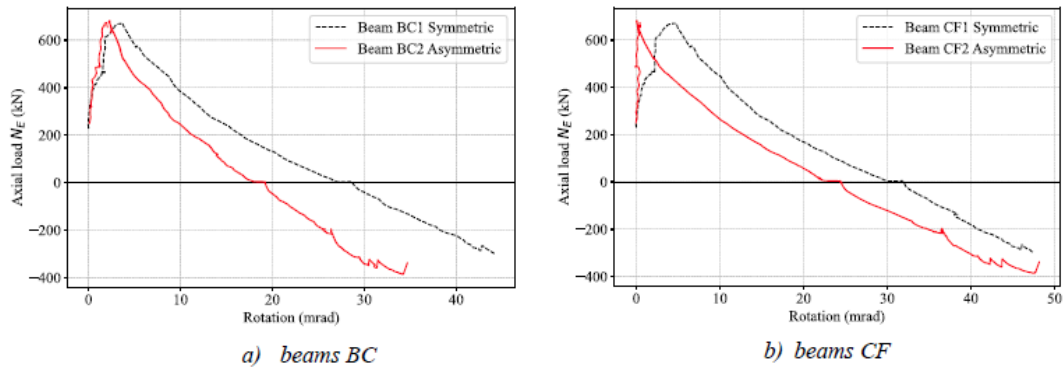


Figure 22. Comparison of the torsional rotation of the beams.

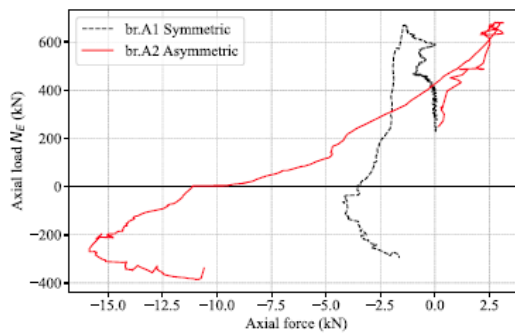
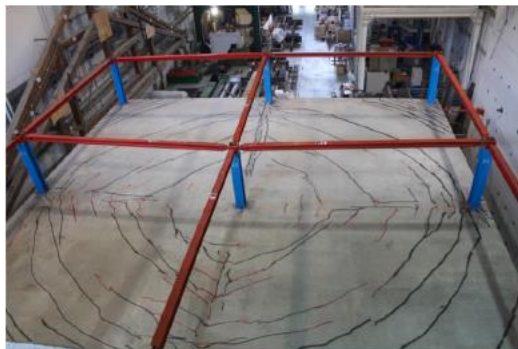


Figure 24. Comparison of the axial force on the restraint br.A (tension positive).



a) Symmetric frame



b) Asymmetric frame

Figure 25. Comparison of the axial force on the restraint br.A (tension positive).

5. Summary and conclusions

This paper presents the main results of an experimental study carried out at the University of Trento in the framework of the ‘ROBUSTIMPACT’ European research project on robustness of steel and concrete composite structures [20]. The Trento study comprises two full-scale tests on 3-D one storey sub-structures subjected to a column loss. The tests aimed at investigating the role of the beam-to-column connections and of the concrete slab in developing alternate load paths, preventing the progressive collapse associated with the central column removal.

The specimens were ‘extracted’ from reference building structures designed according to the Eurocodes with no account for accidental actions (neither earthquake nor robustness). They were characterized by different column layout, symmetric with respect to both plan directions (‘symmetric sub-frame’) and symmetric with respect to the longitudinal direction only (‘asymmetric sub-frame’). The specimens were loaded at the full factored design load and the collapse of the central column, replaced by a hydraulic actuator, was simulated. A tensile force was then applied at the central column location to assess the residual strength of the systems. Both tests were stopped when the structural distress was apparent from the load deflection curve and from the visual inspection of the joints and of the slab. A clear index of the substantial structural deterioration was the fracture of two bolts in one endplate joint of the central node.

The results of the first test (symmetric sub-frame) were reported and discussed in [4]. The aim of this paper is to present the main features and experimental results of the second test (asymmetric sub-frame). The comparison with the results of the symmetric sub-frame is also reported.

The following main outcomes are made from the analysis of the results:

- the load–deflection relationships at the ‘removed column’ did not show any discontinuity associated with the development of catenary action in the beams and membrane action in the slab. However, the analyses of the axial strains and curvatures of the internal beams showed that the trend towards the development of catenary actions. The collapse of the bolts occurred before the full development of such actions. Furthermore, the visual inspection of the slab cracking pattern pointed out the development of the membrane action. The comparison of the two load–deflection relationships (Fig. 18) showed a similar structural behaviour of the two tested frames, although the stiffer response of the asymmetric specimen;
- the joints’ ductility plays a critical role. Both specimens achieved ‘collapse’ due to the fracture of two bolts in the bottom row of a joint in the central column. Lateral joints did not fail, even if important local inelastic deformations occurred. The composite joints designed as ductile under bending, enable development of important plastic rotations (up to 70 mrad) under the combination of tensile axial forces and sagging moments associated with the column removal scenario. An a posteriori check showed that the joints met the requirements provided in the recent literature [33]. In particular, joints were designed to fail (and they failed) in ‘Mode 2’ [25]. A further insight is hence necessary in order to define the range of application of such requirements. Furthermore, enhanced design of the external joints, considering local phenomena, such as local buckling of the bottom beam flange and web, and shear deformation of the column web panel is required;
- the slab significantly contributes to the load redistribution from the damaged to the undamaged parts of the frames, thus allowing a robust structural response. Tests pointed out the role of anchoring the slab to both the lateral beams (Fig. 23) and the external columns (Fig. 11c) to assure the development of its mechanism of resistance. At this aim, it should be provided: i) an efficient anchorage of the slab to the lateral beams by means of shear connectors; ii) a proper detailing of reinforcement bars, such as ‘U’ shaped rebars, to ensure slab-to-column continuity. Further studies should focus on the first issue to define an efficient design criterion;
- the floor asymmetry: i) it doesn’t affect the global behaviour of the tested sub-frames (Fig. 18); ii) it seems to remarkably affect the stress state of internal joints’ increasing the ductility demand in the transverse direction (Fig. 21a) and the strains in the rebars (Fig. 22); iii) it has a limited influence on the redistribution of axial forces in the columns.

Despite a few behavioural differences, both tests showed the significant capability of the sub-frames to respond to the central column loss. The collapse was achieved for a further increment of the load of about 30 %. Therefore, based on the outcomes of these tests, it seems that Eurocodes specifications provide a good base for the design of robust composite steel and concrete frames even if accidental loads are not considered in design. However, a robust response would require specific recommendations of slab and joint detailing.

The tests’ data allowed to calibrate FE Abaqus models and further parametric numerical analysis for better understanding the structural mechanisms and have a further check of the code recommendations [32].

Credit authorship contribution statement

G. Roverso: Validation, Formal analysis, Investigation, Writing – original draft, Visualization. N. Baldassino: Conceptualization, Formal analysis, Investigation, Writing – review & editing, Visualization, Funding acquisition. R. Zandonini: Conceptualization, Investigation, Writing – review & editing, Supervision, Project administration, Funding acquisition. F. Freddi: Validation, Formal analysis, Investigation.

Acknowledgments

The study presented in this paper was made possible by funds of the Research Fund for Coal and Steel of the European Community (Contracts number No. RFSR-CT-2012-00029), which the Authors gratefully acknowledge. The Authors wants also to thank the work of Stefano Girardi, Marco Graziadei and Alessandro Banterla who accomplished the complex and difficult Laboratory work.

References

- [1] Pearson C, Delatte N. Ronan point apartment tower collapse and its effect on building codes. *J Perform Constr Facil* 2005;19(2):172–7.
- [2] National Institute of Standards and Technology – National Construction Safety Team Act (NIST NCSTAR) 2005. Final report on the collapse of the World Trade Center Towers. Washington, DC: U.S. Government Printing Office.
- [3] Demonceau JF, Marginean IM, Golea T, Jaspert JP, Santiago A, Santos AF, *et al.* FAILNOMORE project - D1–2 - background document. RFCS Deliverable 2021.
- [4] Zandonini R, Baldassino N, Freddi F, Roverso G. Steel-concrete frames under the column loss scenario: an experimental study. *J Constr Steel Res* 2019; 162: 105527.
- [5] General Services Administration (GSA). Progressive collapse analysis and design guidelines for new federal office buildings and major modernization projects. Washington, DC; 2003.
- [6] UFC 4-023-03. Design of buildings to resist progressive collapse, Department of Defense (DOD), 2005.
- [7] SEI/ASCE 7-05. Minimum design loads for buildings and other structures. Reston, VA: American society of Civil Engineers; 2005.
- [8] Park R, Gamble WL. Reinforced concrete slabs. 2nd edition. New York: John Wiley & Sons, Inc; 2000.
- [9] Qian K, Li B, Ma JX. Load-carrying mechanism to resist progressive collapse of RC buildings. *J Struct Eng* 2015;141(2):04014107.
- [10] Lim NS, Tan KH, Lee CK. Experimental studies of 3D RC substructures under exterior and corner column removal scenarios. *Eng Struct* 2017; 150: 409–27.
- [11] Pham XD, Tan KH. Experimental study of beam-slab substructures subjected to a penultimate-internal column loss. *Eng Struct* 2013; 55: 2–15.
- [12] Dat PX, Tan KH. Experimental response of beam-slab substructures subject to penultimate-external column removal. *J Struct Eng* 2015;141(7):04014170.
- [13] Pham AT, Lim NS, Tan KH. Investigations of tensile membrane action in beam-slab systems under progressive collapse subjected to different loading configurations and boundary conditions. *Eng Struct* 2017; 150: 520–36.
- [14] Qian K, Li B. Dynamic and residual behavior of reinforced concrete floors following instantaneous removal of a column. *Eng Struct* 2017; 148: 175–84.
- [15] Yu J, Luo L, Li Y. Numerical study of progressive collapse resistance of RC beam- slab substructures under perimeter column removal scenarios. *Eng Struct* 2018; 159:14–27.
- [16] El-Tawil S, Li H, Kunnath S. Computational simulation of gravity-induced progressive collapse of steel-frame buildings: current trends and future research needs. *J Struct Eng* 2014;140(8): A2513001.
- [17] Fu QN, Tan KH, Zhou XH, Yang B. Load-resisting mechanisms of 3D composite floor systems under internal column-removal scenario. *Eng Struct* 2017;148: 357–72.
- [18] Kim S, Lee CH, Lee K. Effects of floor slab on progressive collapse resistance of steel moment frames. *J Constr Steel Res* 2015; 110: 182–90.
- [19] Dimopoulos CA, Freddi F, Karavasilis TL, Vasdravellis G. Progressive collapse resistance of steel self-centering MRFs including the effects of the composite floor. *Eng Struct* 2020; 208: 109923.
- [20] Kuhlmann U, Hoffman N, Jaspert JP, Demonceau JF, Zandonini R, Baldassino N, *et al.* Robust impact design of steel and composite building structures (ROBUSTIMPACT). Final. In: report. Luxembourg: Publications Office of the European Union; 2017.
- [21] EN 1991-1-1. Eurocode 1: Actions on structures – Part 1-1: General actions, densities, self-weight, imposed loads for buildings. Brussels: European Committee for Standardization; 2004.

- [22] EN 1992-1-1. Eurocode 2: Design of concrete structures – Part 1-1: General rules and rules for buildings. Brussels: European Committee for Standardization; 2004.
- [23] EN 1993-1-1. Eurocode 3: Design of steel structures – Part 1-1: General rules and rules for buildings. Brussels: European Committee for Standardization; 2005.
- [24] EN 1994-1-1. Eurocode 4: Design of composite steel and concrete structures – Part 1-1: General rules and rules for buildings. Brussels: European Committee for Standardization; 2004.
- [25] EN 1993-1-8. Eurocode 3: Design of steel structures – Part 1-8: Design of joints. Brussels: European Committee for Standardization; 2005.
- [26] Baldassino N, Freddi F, Zandonini R. Moment resisting steel-concrete composite frames under the column loss scenario: design of the reference frames and of the full-scale sub-frame specimens. University of Trento: Research report of the Department of Civil, Environmental and Mechanical Engineering; 2018.
- [27] EN 12390-2. Testing hardened concrete – Part 2: Making and curing specimens for strength tests. Brussels: European Committee for Standardization; 2009.
- [28] EN 12390-3. Testing hardened concrete – Part 3: Compressive strength of test specimens. Brussels: European Committee for Standardization; 2009.
- [29] EN 12390-6. Testing hardened concrete – Part 6: Tensile splitting strength of test specimens. Brussels: European Committee for Standardization; 2010.
- [30] UNI 6556. Prove sui calcestruzzi. Determinazione del modulo elastico secante a compressione. Milano: Ente Nazionale Italiano di Unificazione; 1976.
- [31] EN ISO 376. Metallic materials - Calibration of force-proving instruments used for the verification of uniaxial testing machines. Brussels: European Committee for Standardization; 2011.
- [32] Roverso G. Progressive collapse assessment of steel and concrete composite structures subjected to extreme loading conditions. University of Trento; 2019. PhD thesis, XXXI cycle.
- [33] Demonceau JF, Golea T, Jaspard JP, Elghazouli A, Khalil Z, Santiago A, *et al.* Design recommendations against progressive collapse in steel-concrete buildings (Failnomore). Brussels: ECCS-. European Convention for Constructional Steelwork 2021.